A Study on Structural and Optical Properties of Nanostructure $Mg_xZn_{1-x}O$ Thin Films Using Pulsed Laser Deposition

Dr. Ali A. Yousif
Education College, University of Al-Mustansiriyah/ Baghdad
Email: aliyousif73@gmail.com
Marwa A. Abd-Majeed
Education College, University of Al-Mustansiriyah/ Baghdad

Received on: 23/7/2013 & Accepted on: 23/4/2014

ABSTRACT

For this paper, films have been grown under various deposition conditions in order to understand the effect of processing on the film properties and to specify the optimum condition, namely substrate at temperatures of 400°C, oxygen pressure (2×10^{-1}) mbar, laser fluence 400 mJ, and with different Mg doping (x=0, 0.02, 0.04, 0.06), using double frequency Q-switching Nd:YAG laser beam (wavelength 532nm), repetition rate (1-6) Hz and the pulse duration of (10 ns), to deposit $Mg_xZn_{1-x}O$ films on glass substrates with thickness of about 200±10 nm for all $Mg_xZn_{1-x}O$ films at different deposition condition and the number of laser pulses was 100 pulses. The X-rays spectra revealed that the presence of diffraction peaks indicates that the polycrystalline of the films depended strongly on the Mg-content in the layers. All the grown films is (101) as predominant reflection**.** The Scanning Electron Microscopy (SEM) images, the average grain size less than 50 nm. From the study of atomic force microscopy (AFM), we can determine the root mean square (RMS) surface roughness of Mg doped ZnO films**.** The optical properties were characterized by the transmittance and absorption spectroscopy at room temperature, measured in the range from (300 - 900) nm. For all the films, the average transmittance in the visible wavelength region λ = (400 - 800) nm is greater than (70%). The maximum value of the transmittance is greater than (95%) was obtained for these films. (E_g) values of $Mg_xZn_{1-x}O$ thin films are (3.37, 3.59, 3.82, and 4)eV corresponding to the Mg-content (x = 0, 0.02, 0.04 and 0.06) respectively. In other word, the optical band gap of $Mg_xZn_{1-x}O$ thin films become wider as Mg-content increases and can be precisely controlled between 3.37 and 4eV.

Keywords: Zinc oxides, pulsed laser deposition, structural and optical properties, $Mg_xZn_{1-x}O$.

دراسة الخصائص التركيبية والبصرية للاغشية الرقيقة ZnO المشوبة ب Mg ذات التراكيب النانوية باستخدام تقنية الليزر النبضي

الخلاصـــة

تم في هذا البحث دراسة نمو الاغشية بظروف ترسيب مختلفة لفهم تاثير طريقة التحضير على خصائص الغشاء و لتحديد افضل الظروف التحضيرية وتتمثل بدرجة الحرارة 400°C, وضغط

الاوكسجين mbar (2×10^{-1}), كثافة طاقة الليزر الساقطة 400mJ وباختلاف تشويب المغنيسيوم (x=0, 0.02, 0.04, 0.06) باستخدام التردد المضاعف لليزر النيديميوم- ياك والذي يعمل بتقنية عامل النوعية عند الطول الموجي 532nm بمعدل تكرارية (6 – 1) هرتز وامد نبضة 10 نانوثانية لترسيب اغشية اوكسيد الخارصين المشوب بلمغنيسيوم $Mg_xZn_{1-x}O$ على قواعد من الزجاج بسمك 200±10نانومتر وعدد نبضات 100 نبضة لكل الاغشية باختلاف ظروف الترسيب. أطياف الأشعة السينية اثبتت بأن نتائج قمم الحيود تشيرالى ان درجة التبلور للاغشية تعتمد بقوة على كمية المغنيسيوم في الطبقات. جميع الأغشية المنماة تمتلك المستوي (101) كانعكاس سائد هي أغشية ذات تركيب سداسي متعددة التبلور يكون فيها المستوي (101) هو المستوي السائد. قياسات المجهر الالكتروني الماسح فقد وجد ان معدل الحجم الحبيبي كان اقل من 50 نانومتر . من دراسة مجهر القوى الذرّيه نسطيع أن نحدد مربع الجذر المتوسط (RMS) لخشونة سطح اغشية اوكسيد الخارصين المشوبة بالمغنيسيوم. الخصائص البصرية تمت دراستها بوساطة قياس طيف النفاذية والامتصاصية عند درجة حرارة الغرفة, لمدى طول موجي يتراوح من nm (900 - 300) . معدل النفاذية لجميع الأغشية للمنطقة المرئية من الطيف nm (800 - 400) = λ تكون اكبر من (% 70) وتصل في احدى النماذج لاكثر من (% 95) . ان قيم فجوة الطاقة (E_g) لهذه الأغشية تساوي (3.37, 3.59, 3.82, 4) الكترون- فولت لكل من التراكيز (x = 0, 0.02, 0.04, 0.06) على التوالي. كما ان قيم فجوة الطاقة تزداد بزيادة نسبة المغنيسيوم في الأغشية ويمكن التحكم بقيمة فجوة الطاقة بالضبط بين (3.37 و 4) الكترون – فولت.

INTRODUCTION

In recent years, studies on synthesis, characterization, and applications of ZnO nanostructures [1] have been studied extensively, because ZnO nanostructures have been regarded as a promising nanomaterial in a wide range of applications like solar cells, sensors, light-emitting diodes, piezoelectric nanogenerators, field-effect transistors, and transparent electrodes [2]. Zinc oxide is II–VI compound semiconductor with a wide direct band gap (3.37eV at room temperature) and a hexagonal wurtzite structure (space group P63mc with cell parameters (a= 3.25 Å, c = 5.207 Å) [3]. ZnO films can be grown by many deposition techniques, such as magnetron sputtering [4], chemical vapor deposition (CVD) [5], spray pyrolysis [6], pulsed laser deposition (PLD) [7], molecular beam epitaxy (MBE) [8], sol–gel [9], and so forth. ZnO thin films and nanostructures are widely used in various applications which include light emitting diodes (LED), UV photo detectors, transparent conducting oxides (TCOs), transparent thin film transistors (TTFTs), solar cells windows, piezoelectric transducers, Gas Sensors etc.. The large exciton binding energy makes ZnO a promising material for optical devices that are based on exciton effects. Due to a strong luminescence in the green–white region of the spectrum, ZnO is also a suitable material for phosphor applications. [10]

The aims of this work to reveal specific properties of $Mg_xZn_{1-x}O$ thin films nanocrystalline materials. Initially the series of samples have been prepared by pulsed laser deposition technique at different technological conditions on glass substrates. That supposed to result in the different structural properties, different surface morphology of the nanostructures to be obtained, also the optical properties.

Experiment

The nanostructures $Mg_xZn_{1-x}O$ films were prepared by employing pulsed laser deposition experiment under vacuum conditions (10^{-3} Torr). Nd:YAG laser (**Huafei Tongda Technology**—DIAMOND-288 pattern EPLS) is used for the deposition of ZnO films on different substrate. The whole system is consisting of light route

system, power supply, computer controlling and cooling systems. The light route system is installed into the hand piece, while the power supply, controlling and cooling system are installed into the machine box of power supply.

X-ray power diffraction (XRD) is one of the most powerful techniques for qualitative and quantitative analysis of crystalline compounds. This experimental technique has long been used to determine the overall structure of bulk solids, including lattice constants, identification of unknown materials, orientation of single crystals, orientation of polycrystals, defects, stresses, etc. In this study X-ray diffractrometer type SHIMADZU, power diffraction system with Cu-Kα X-ray tube (λ = 1.54056 Å) is used. The X-ray scans are performed between 2θ values of 20° and 70°.

The SEM study carried out by (FEL Quanta 200, Netherlands) scanning electron microscope equipped with Energy dispersive X-ray (EDAX). The operation principle of an AFM the consists of a cantilever and a sharp tip at its end. The surface of the specimen is scanned with the tip. The distance between the specimen surface and the tip is short enough, to allow the van der Waals forces between them to cause deflection of the cantilever. The deflection follows Hooke's law and the spring constant of the cantilever is known, thus the amount of deflection and further, the topographical profile of the specimen, can be determined. Typically, the deflection is measured using a laser spot reflected from the back surface of the cantilever into an array of photodiodes.

The optical transmittance of $Mg_xZn_{1-x}O$ thin films with different doping concentrations (x = 0, 0.02, 0.04, 0.06) on glass substrates with different deposition condition, by using spectrophotometer (SHIMADZU UV- 1650 PC), for the wavelength range from 300 nm to 900 nm. The optical properties are calculated from these optical measurements.

Results and Discussion

The results and discusses the effect of doping, upon the characterization such as structural and optical properties of the films grown by PLD, also the structural measurements such as, morphological features by Scanning Electron Microscopy (SEM), Atomic Force Microscope (AFM).

Structural Properties

X-ray Diffraction:

Figures (1), shows the X-ray diffraction profiles of $Mg_xZn_{1-x}O$ thin films deposited at a temperature of ($400\,^0C$) for different magnesium content, x. The presence of diffraction peaks indicates that the film is polycrystalline with a hexagonal wurtzite type crystal structure and no amorphous phase is detected. It is revealed that the sprayed film has peaks corresponding to (100), (002), (101), (102), (110) and (112), directions of the hexagonal ZnO crystal structure which is corresponding to the positions $2q$ = 31.7741^0, 34.4424^0, 36.2497^0, 47.5794^0, 55.57^0 and 67.44^0 respectively. The (d) value, that is the interplanar spacing of (101) plane of the film was evaluated from the position of (101) peak from the XRD data. The observed (d) value is 2.471 which is in excellent agreement with the standard (d) value $2.476A^0$ taken from the (ASTM) and the position of (101) peak taken from the XRD pattern is 36.31^0 which is in agreement with the standard value 36.253^0 taken from (ASTM), as shown in table (1)

Table (1) XRD parameters of ASTM and prepared $Mg_xZn_{1-x}O$ thin films

Concentration(x)			ZnO	$Mg_{0.02}Zn_{0.98}O$	$Mg_{0.04}Zn_{0.96}O$	$Mg_{0.06}Zn_{0.94}O$	ASTM for ZnO
hkl	100	2Θ(deg)	31.69	31.73	31.75	31.9	*
		θ(deg)	15.845	15.865	15.875	15.95	*
		d(Å)	2.8201	2.8205	2.815	2.805	2.816
	002	2Θ(deg)	34.42	34.45	34.47	34.48	*
		θ(deg)	17.21	17.225	17.235	17.24	*
		d(Å)	2.601	2.605	2.599	2.598	2.602
	101	2Θ(deg)	36.31	36.31	36.34	36.41	36.253
		θ(deg)	18.155	18.155	18.17	18.205	*
		d(Å)	2.471	2.471	2.469	2.467	2.476
	102	2Θ(deg)	47.54	47.48	47.45	47.62	*
		θ(deg)	23.77	23.74	23.725	23.81	*
		d(Å)	1.910	1.913	1.915	1.908	1.911
	110	2Θ(deg)	55.55	55.52	55.62	55.48	*
		θ(deg)	27.775	27.76	27.81	27.74	*
		d(Å)	1.652	1.654	1.650	1.655	1.626
	112	2Θ(deg)	67.70	67.77	67.66	67.58	*
		θ(deg)	33.85	33.885	33.83	33.79	*
		d(Å)	1.382	1.381	1.383	1.384	1.379

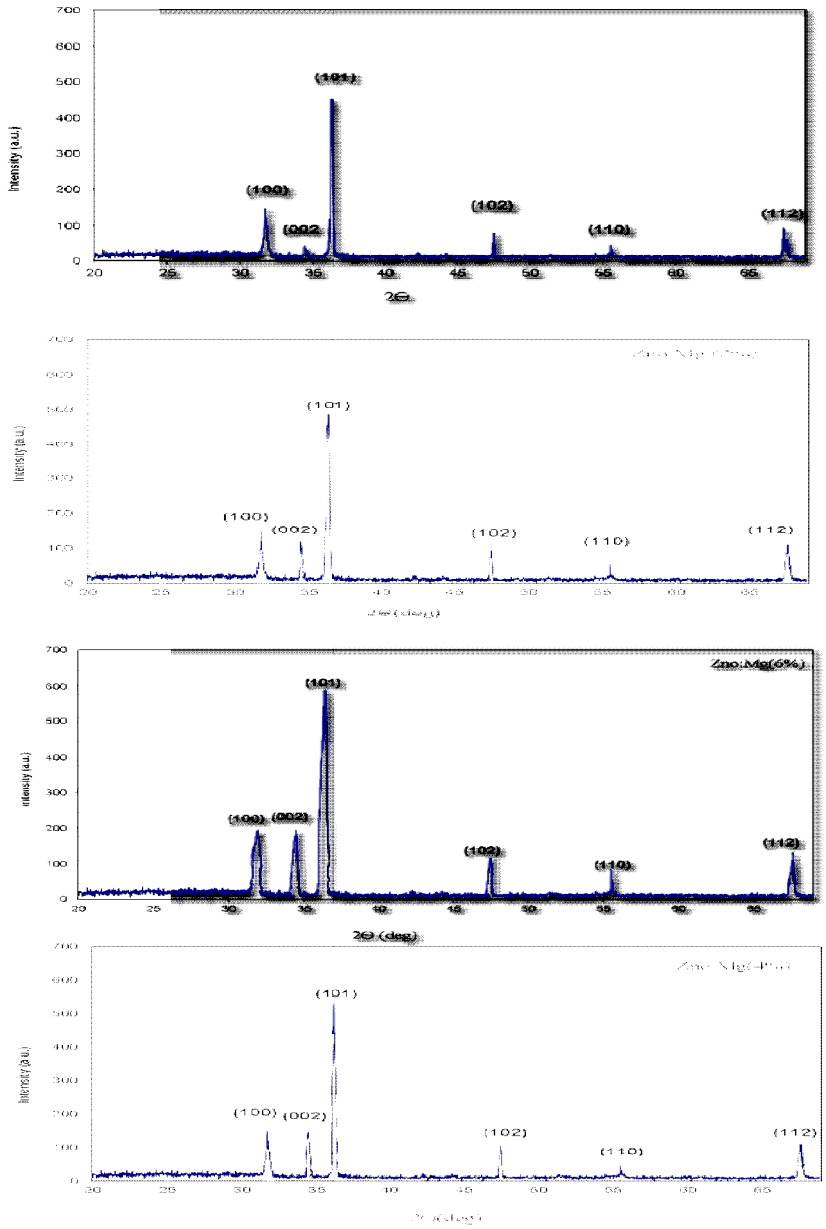

Figure (1). XRD patterns of pure ZnO films with various Mg-content (x=0, x=0.02, x=0.04 and x=0.06) grown on glass substrates at temperature 400°C.

The X-ray diffraction data revealed that the crystallinity of the films depended strongly on the Mg-content in the layers. All the grown films of ZnO pure and doping (101) as predominant reflection were polycrystalline with reflection along with the other (100), (002), (102), (110) and (112), reflections that corresponding to the hexagonal wuartzite-type nanostructure of ZnO films. [11]. For all the $Mg_xZn_{1-x}O$ films , the angle position of the (101) peak moves toward greater values with

increasing Mg-content, which indicates that Zn^{2+} ions are successfully substituted by Mg^{2+} in the ZnO lattice , which is in agreement with another reports [11].

On the other hand we can observe that the intensity of (101) peaks increases with increasing Mg-content whereas (002) peaks also become more intense as the Mg-content increases, which is consistent with the another report [12].

The lattice constant a and c for the prepared ZnO thin film are (3.256 Å) and (5.204Å) respectively , that is in a good agreement with the standard values (3.249 Å) and (5.205Å) taken from (ASTM) card file data. This indicates that the degree of nanocrystalinity increase with increasing Mg-content in the film. The lattice constants and the relative intensity ratio, in the diffraction pattern of $Mg_xZn_{1-x}O$ films are given in table (2). The lattice constants obtained are found to be in good agreement with (ASTM). [13]

Table (2) Lattice constants of $Mg_xZn_{1-x}O$

sample	a_o(Å)	c_o (Å)	d(Å)	hkl
ASTM	**3.249**	**5.205**	**2.816 2.602 2.476 1.911 1.626 1.379**	**100 002 101 102 110 112**
ZnO-pure	**3.2563**	**5.204**	**2.8201 2.602 2.475 1.913 1.652 1.382**	**100 002 101 102 110 112**
$Mg_{0.02}Zn_{0.98}O$	**3.2568**	**5.202**	**2.8205 2.601 2.471 1.910 1.654 1.381**	**100 002 101 102 110 112**
$Mg_{0.04}Zn_{0.96}O$	**3.250**	**5.20**	**2.815 2.599 2.469 1.915 1.650 1.383**	**100 002 101 102 110 112**
$Mg_{0.06}Zn_{0.94}O$	**3.238**	**5.196**	**2.805 2.598 2.467 1.908 1.655 1.384**	**100 002 101 102 110 112**

The values of full width at half maximum (FWHM) of the preferred orientation ((101) for ZnO pure and ZnMgO) are increase with increasing Mg-content in the film as shown in table (3). This indicates that the grain size decreases with increasing Mg-content. [14]

The values of the structural parameters from XRD data for $Mg_xZn_{1-x}O$ thin films for ($0 \le x \le 0.06$) are listed in table (3).

The values of the full width at half maximum (FWHM) increases from 0.1622° for *x*=0 (pure ZnO) to 0.281° for ($Mg_{0.06}Zn_{0.94}O$) as Mg content increased. The average grain size of $Mg_xZn_{1-x}O$ films prepared at different Mg-content (x = 0 , 0.02 , 0.04, 0.06) was calculated using the fringe width at half maximum (FWHM) of the films using Scherrer formula. The film prepared at ZnO pure, (x = 0) showed the highest crystallite size of (52 nm) and its value decreases with increasing Mg-content as shown in table (3). Also the XRD peaks can be widened (FWHM increase) by internal stress and defect when increasing Mg-content in the films, so the grain size decreases with increasing Mg-content. [15] The micro strain depends directly on the lattice constant (c) and its value related to the shift from the (ASTM) standard value. The values of micro strain increase with increasing Mg-content in the films as shown in table (3). The calculation of the film stress is based on the strain model, as shown in table (3). This strain and stress can be calculated from the formulas: [13]

$$S_n = \left[\frac{|C_{ASTM} - C_{XRD}|}{C_{ASTM}} \right] \times 100\% \qquad \text{…. (1)}$$

The residual stress (S_s) in ZnO films can be expressed as [13]

$$S_s = \frac{2c^2{}_{13} - c_{33}(c_{11} + c_{12})}{2c_{13}} \times \frac{c - c_O}{c_O} \qquad \text{…. (2)}$$

Here c_{ij} is the elastic stiffiness constant for single crystal ZnO (where c_{11}=208.8 GPa, c_{33}=213.8 GPa, c_{12}=119.7 GPa and c_{13}=104.2 GPa [13].

To describe the preferential orientation, the texture coefficient, TC (hkl) is calculated using the expression [13]:

$$Tc(hkl) = \frac{[(I(hkl)/I_o(hkl)]}{[Nr^{-1}\sum I(hkl)/I_o(hkl)]} \qquad \text{…. (3)}$$

Where:

I : is the measured intensity .
I_o : the ASTM standard intensity .
Nr : the reflection number .
(hkl) : Miller indices

Texture coefficient (Tc) of ZnO thin films, the results indicate that (Tc) decrease with increasing doping with Mg concentration. This is a usual result because increased doping causes an increase in the surface roughness. [15]

Table (3) The Size – strain data of investigated thin films

sample	Investigated line	FWHM (deg)	Grain size g.s(nm)	Strain Sn(%)	Stress Ss	Texture Coefficient (Tc)
ZnO	101	0.1622	52	0.0192	-0.0446	1.732
$Mg_{0.02}Zn_{0.98}O$	101	0.1860	47	0.0576	-0.1340	1.65
$Mg_{0.04}Zn_{0.96}O$	101	0.2133	40	0.0960	-0.223	1.706
$Mg_{0.06}Zn_{0.94}O$	101	0.281	31	0.153	-0.356	1.54

Scanning Electron Microscopy (SEM)

SEM is a promising technique for the topography study of samples, as it provides valuable information regarding the growth mechanism, shape and size of particles and/or grains [16].

Figures (2) to (5) show the SEM micrographs of $Mg_xZn_{1-x}O$ thin films (x = 0, 0.02, 0.04, 0.06), with a average magnifications of (500-50000 X). From these pictures, it can be observed that $Mg_xZn_{1-x}O$ thin films consist of spherically nanosized grains of nearly regular size and covered the entire surface of the substrates. All films compactness is high and the surface's uniformity (homogeneity) is good without defects or cracks. the particle size is quite fine. The grain size is measured by keeping the SEM photograph under traveling microscope. The average grain size in the micrograph calculated to be approximately less than 50 nm.

It is observed that with increase Zn^{2+} content from x=0.04 to x=0.06 the grain size decreases as shown in figure (4) and (5), while at x=0 and x=0.02 the differences in grain sizes are very small, as shown in figure (2) and (3). On the deposited films, bigger size of particles seems bright may be due to agglomeration of nanoparticles were scattered electrons in the same phase. The crystallite size obtained from XRD Scherrer's equation is lower than the observed value from SEM. The differences between them may be due to the average size of crystallites obtained from XRD whereas from Atomic force microscopy (AFM), the obtained sizes are from the surface of the grains, this agrees with, M. Salina et al. [17]. However, these characteristics are in good agreement with the films high transparency.

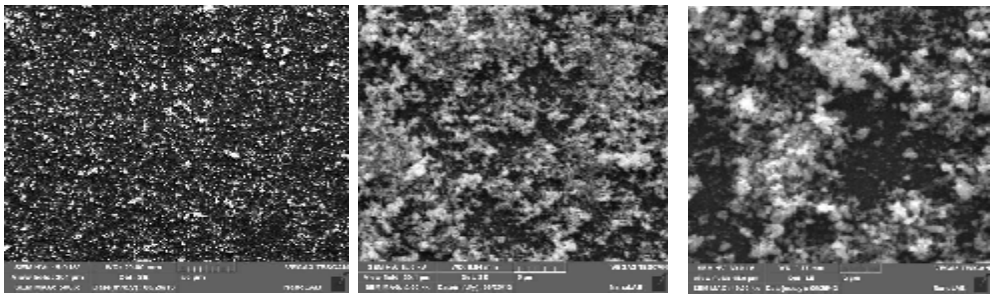

Figure (2), (SEM) surface morphology of ZnO-pure, a)- (500X), b)- (5000X), c)- (10000X)

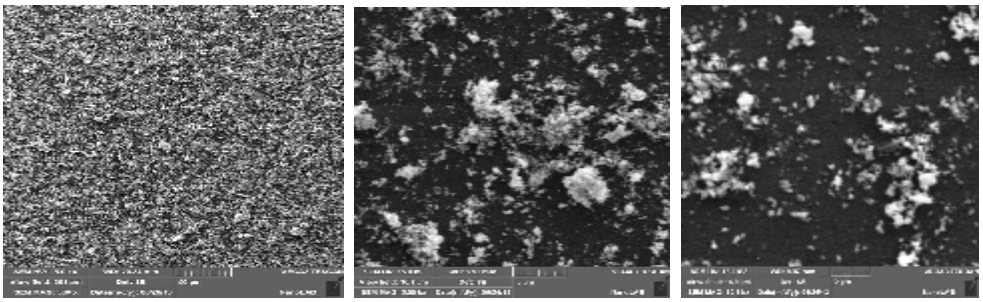

Figure(3), (SEM) surface morphology of $Mg_{0.02}Zn_{0.98}O$, a)- (500X),b)- (5000X), c)-(10000X)

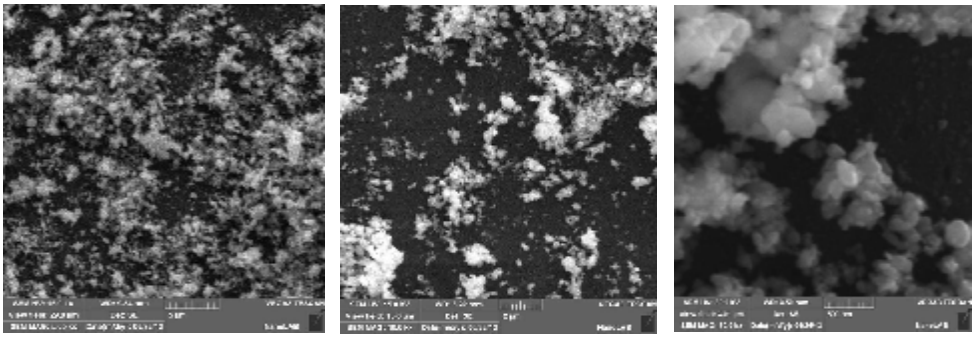

Figure (4) (SEM) surface morphology of $Mg_{0.04}Zn_{0.96}O$,a)- (5000X) b)- (10000X) c(50000X)

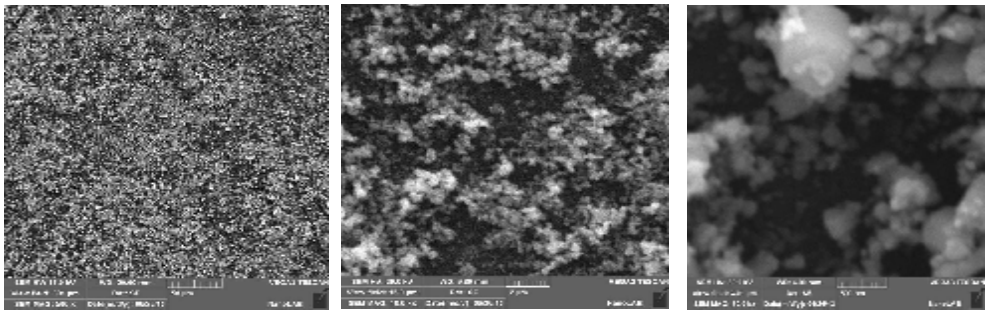

Figure (5), (SEM) surface morphology of $Mg_{0.06}Zn_{0.94}O$, a)- (5000X), b)- (10000X), c)-(50000X)

Atomic Force Microscopy (AFM)

Atomic force microscopy (AFM) technique is a useful method analysis of the surface topography of the thin films. Figures (6) shows two and three dimensional AFM images for the $Mg_xZn_{1-x}O$ thin films deposited on glass substrate temperature 400 ^oC, oxygen pressure 2×10^{-1} mbar, and laser fluence 0.4 J/cm^2 using different Mg contents (x= 0, 0.02, 0.04 and 0.06) with scaning area (10 × 10 µm^2) that showed the variation of surface roughness with Mg-content in the layers. As can be noticed from this figures, the nanocrystalline $Mg_xZn_{1-x}O$ films has high degree of homogeneity and the small grains has uniform distribution on the substrate. Root mean square (RMS) values are (56.6, 54.8, 44.9 and 39.4 nm) with (x= 0, 0.02, 0.04 and 0.06) respectively. It is found from the AFM studies that the Root mean square (RMS) and surface roughness average of the films decreases with increasing the Mg content. This is in agreement with the work of L. W. Ji et. al. [18]. On the other hand, root mean square (RMS) roughness is defined as the standard deviation of the surface height profile from the average height, is the most commonly reported measurement of surface roughness. The root mean square (RMS), the average roughness and maximum height of the deposited $Mg_xZn_{1-x}O$ thin films are shown in the table (4).

Table (4): Morphological characteristics from AFM images for $Mg_xZn_{1-x}O$ thin film.

Mg-content	Root Mean Square (RMS) (nm)	Roughness average (nm)	Ten Point Height (nm)
ZnO	56.6	36.2	457
$Mg_{0.02}Zn_{0.98}O$	54.8	41.9	388
$Mg_{0.04}Zn_{0.96}O$	44.9	31.4	445
$Mg_{0.06}Zn_{0.94}O$	39.4	29.6	348

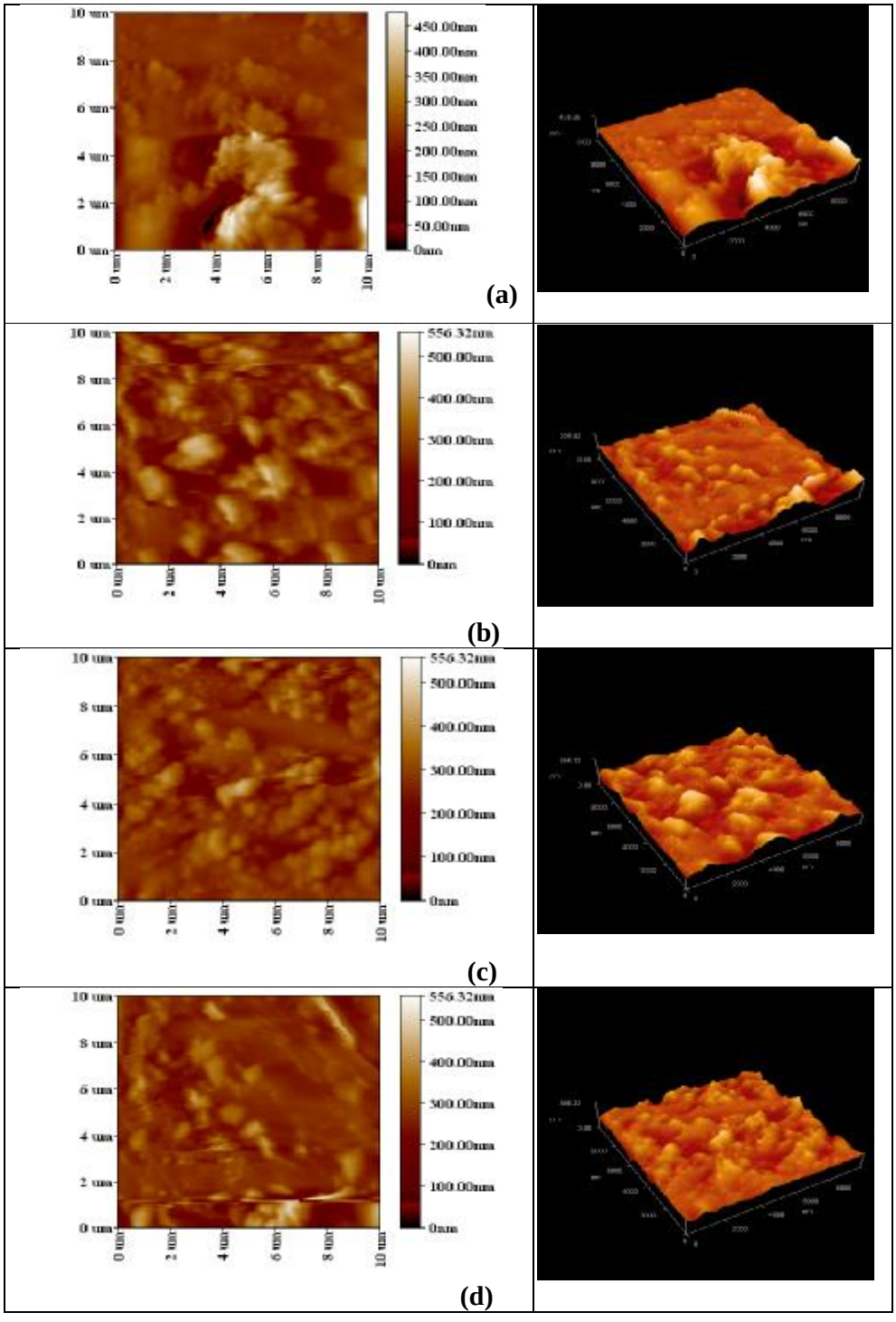

Figure.(6): 2D and 3D AFM images of $Mg_xZn_{1-x}O$ films deposited at 400 °C temperature with different Mg contents a) x=0, b) x=0.02, c) x=0.04 and d) x=0.06.

Optical Properties

The optical properties of the pure $Mg_xZn_{1-x}O$ films deposited by pulsed laser deposition technique are measured by UV-VIS spectrophotometer on glass substrate at 400 °C temperature in the range from 300nm to 900nm. The laser fluence energy density is 0.4 J/cm^2 and the oxygen pressure is maintained at $2x10^{-1}$ mbar various Mg-content(x=0, x=0.02, x=0.04 and x=0.06) with film average thickness 200 nm. The absorptance and transmittance have been studied. Also the optical energy gap and optical constants have been determined.

Transmittance (T)

transmittance spectra of $Mg_xZn_{1-x}O$ thin films deposited on glass wit The optical transmittance of the fig. (7), shows the UV/visible h different Mg-contents. The transmittance spectra of the films can be analyzed as follows:

1. For all the films, the average transmittance in the visible wavelength region λ=(400-800)nm is greater than (80%). The maximum value of the transmittance is greater than (95 %) was obtained for at concentration increasing of doping (x=0.06) these films.
2. The slope of the absorption edge are gone up and there is an obvious shift of the absorption edge to the shorter wavelength with increasing Mg-content The Observed shift in the absorption edge towards the blue region clearly reflects the incorporation of Mg in the ZnO lattice, indicating that the optical band gap was enlarged by Mg doping regardless of crystallinity which is in agreement with the report [19].
3. The transmittance of the $Mg_xZn_{1-x}O$ thin films increases with increasing Mg-content in the films, and when the transmittance increases the grain size decrease,which is consistent with another report [20].

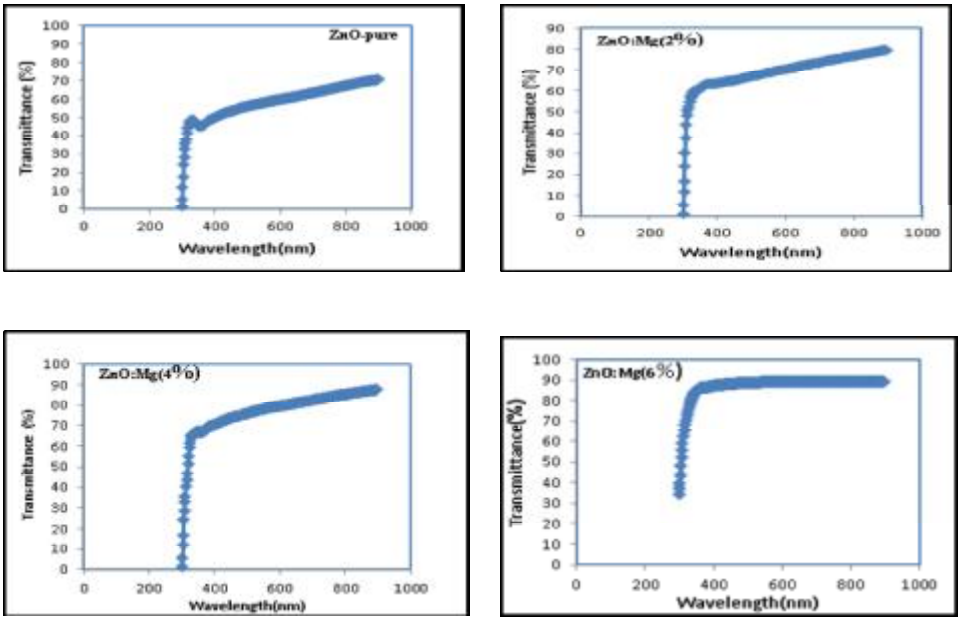

Figure. (7): The optical transmission of ZnO thin films with various Mg-content(x=0, x=0.02, x=0.04 and x=0.06)

Optical Absorption Coefficient (α)

Fig. (8) shows the absorption coefficient (α) of the $Mg_xZn_{1-x}O$ thin films with different Mg-contents determined from transmittance measurements. The absorption coefficient of $Mg_xZn_{1-x}O$ thin films decreased sharply in the UV/VIS boundary, and then decreased gradually in the visible region because it is inversely proportional to the transmittance. The absorption coefficient is decreasing with the increase of Mg-concentration, its value is larger than (10^4 cm^{-1}). This can be linked with decrease in grain size and it may be attributed to the light scattering effect for its low surface roughness [21].

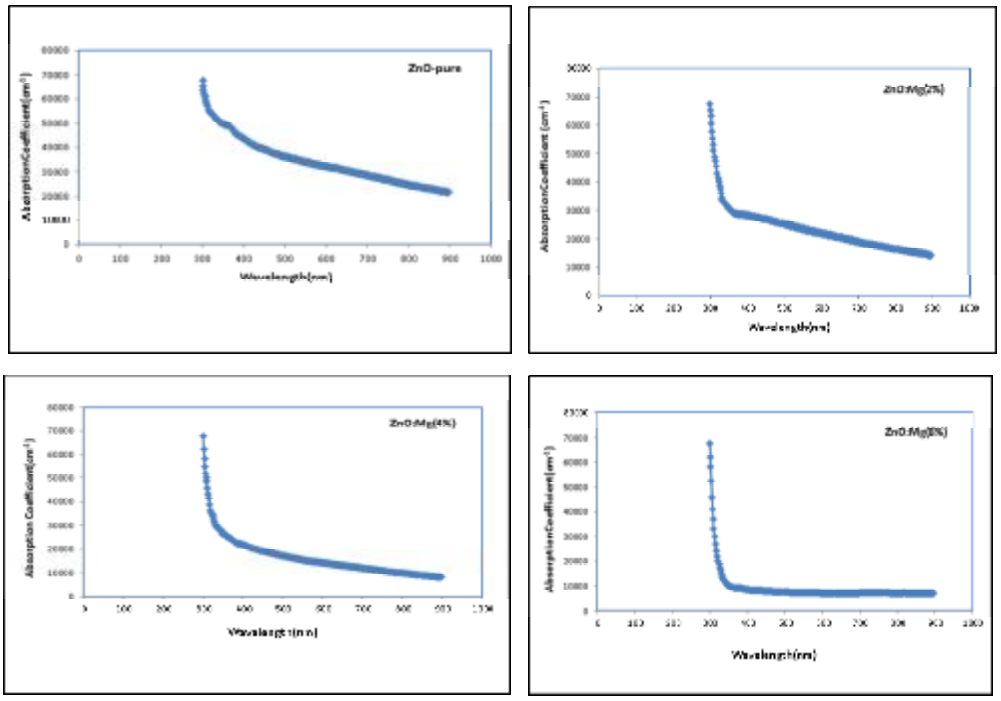

Figure. (8) Absorption coefficient as a function of wavelength of $Mg_xZn_{1-x}O$ thin films at different Mg-content

Optical Energy Gap (E_g)

The optical band gap (E_g) of the $Mg_xZn_{1-x}O$ thin films was evaluated from the transmission (or absorption) spectra and the optical absorption coefficient (α) near the absorption edge for allowed direct transitions. The characteristics of $(ahn)^2$ vs. hn (photon energy) were plotted for evaluating the band gap (E_g) of the $Mg_xZn_{1-x}O$ thin films, and extrapolating the linear portion near the onset of absorption edge to the energy axis as shown in Fig. (9).

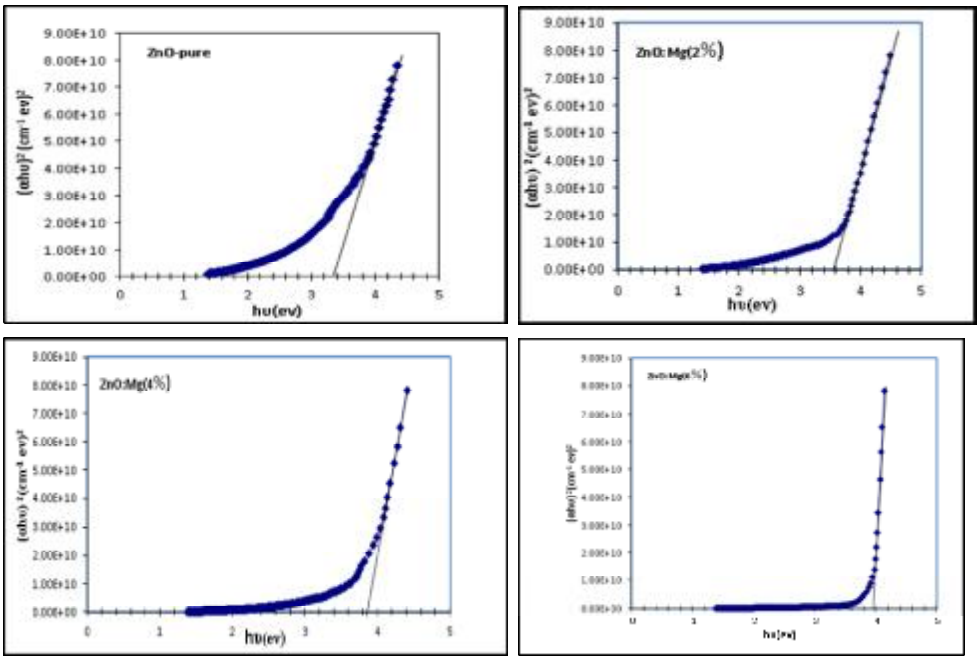

Figure. (9) Variation of $(ahn)^2$ vs. photon energy (hn) for ZnO:Mg thin film.

As can be seen clearly, Eg values of $Mg_xZn_{1-x}O$ thin films are (3.37, 3.59, 3.82 and 4) corresponding to the Mg-concentrations (x = 0, 0.02, 0.04 and 0.06) respectively, which shows in table (5). In other word, the optical band gap of $Mg_xZn_{1-x}O$ thin films become wider as Mg-content increases and can be precisely controlled between 3.37 and 4eV, which is consistent with the reports [22-27].

Table (5): The values of optical energy gap for $Mg_xZn_{1-x}O$ thin film.

Mg-content	Eg (eV) at T=400°C, E=400mJ
ZnO	**3.37 eV**
$Mg_{0.02}Zn_{0.98}O$	**3.59 eV**
$Mg_{0.04}Zn_{0.96}O$	**3.82 eV**
$Mg_{0.06}Zn_{0.94}O$	**4.00 eV**

Reflectance (R)

Fig. (10), shows the reflectance spectra of $Mg_xZn_{1-x}O$ thin films measured at room temperature. The reflectance of $Mg_xZn_{1-x}O$ films decreased with the increase of Mg-concentration in the films and especially at concentration increasing of doping (x=0.06).

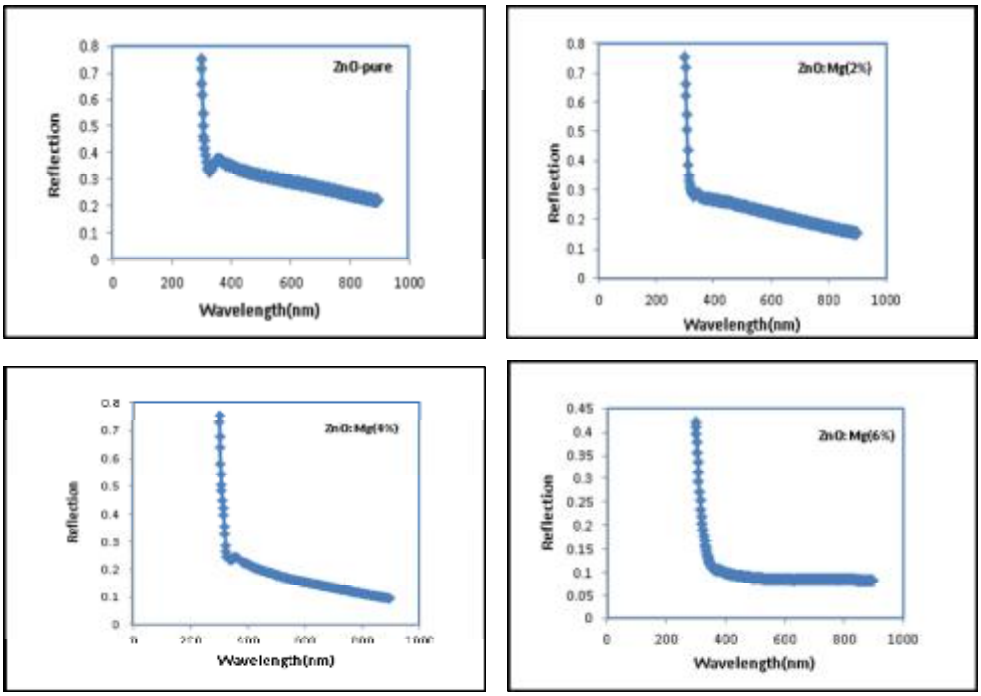

Figure. (10): The optical Reflectance of ZnO thin films with various Mg-content (x=0, x=0.02, x=0.04 and x=0.06)

Refractive Index (n)

The refractive indices (n) of the $Mg_xZn_{1-x}O$ thin films, As shown in Fig.(11), the refractive indices of the films are influenced by the Mg-content. The refractive indices decrease as the Mg-content increases in the range of (1.5 - 2.6) respectively. And the refractive index decrease as the wavelength increases, in our research the decreases in grain size with the decreasing of refractive index is observed. The decrease of refractive index and absorption index may be due to the improvement of stoichiometry [20], the decrease in grain size and the increase in micro strain, which is consistent with other reports [28, 29].

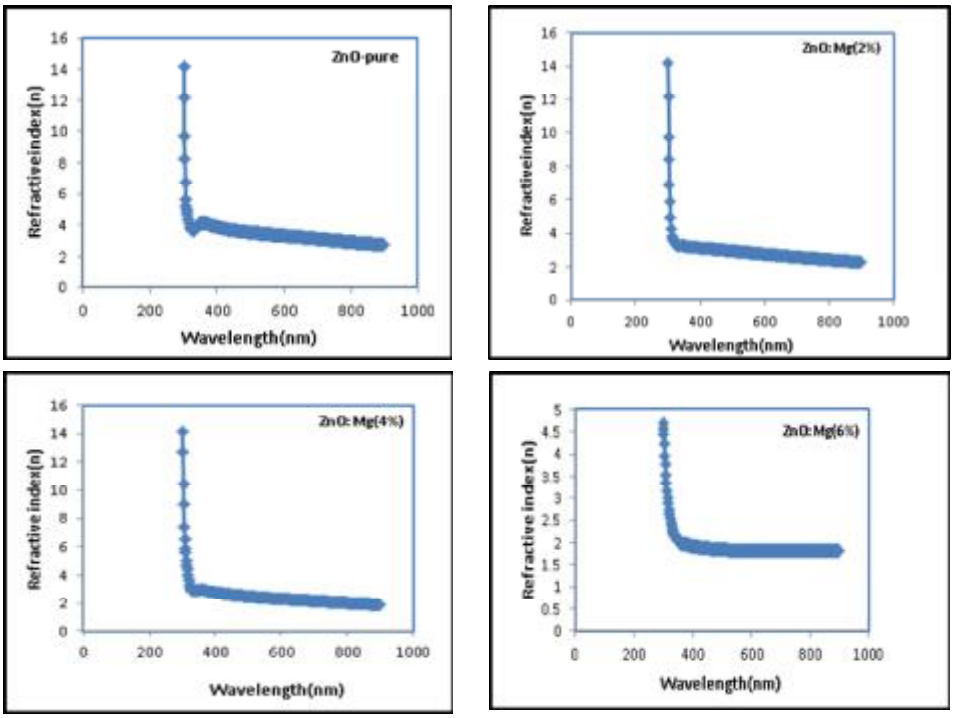

Figure. (11) Refractive index as a function of wavelength for $Mg_xZn_{1-x}O$ thin films at different Mg-content

Extinction Coefficient (K_o)

Fig. (12) shows the extinction coefficient (K_0) as a function of wavelength for different Mg-content. The extinction coefficient of the films is influenced by the Mg-content. The extinction coefficient decrease as the Mg-content increases. And the extinction coefficient decrease as the wavelength increases, which is consistent with other reports [20, 28, 29]

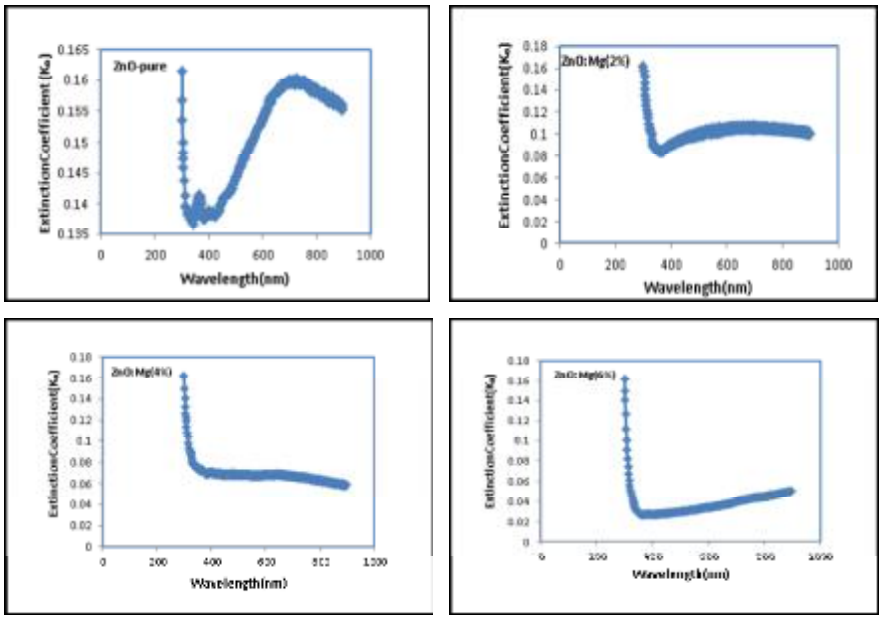

Figure.(12) Extinction coefficient as a function of wavelength for $Mg_xZn_{1-x}O$ thin films at different Mg-content.

Real and Imaginary Part of Dielectric Constant (ε_r), (ε_i)

An absorbing medium is characterized by a complex dielectric constant. The real and imaginary part of dielectric constant of the $Mg_xZn_{1-x}O$ thin films deposited on glass substrate by Pulse laser deposition technique , as shown in Figs. (13)(14). The variation of (ε_r), (ε_i) with wavelength for percentage of both types of pure ZnO and ZnO:Mg films. The obtained results show that the values of real and imaginary part of dielectric constant are decreased with increasing of wavelength for $Mg_xZn_{1-x}O$ thin films, especially it decreased with rate of concentration increasing of doping (x=0.06).

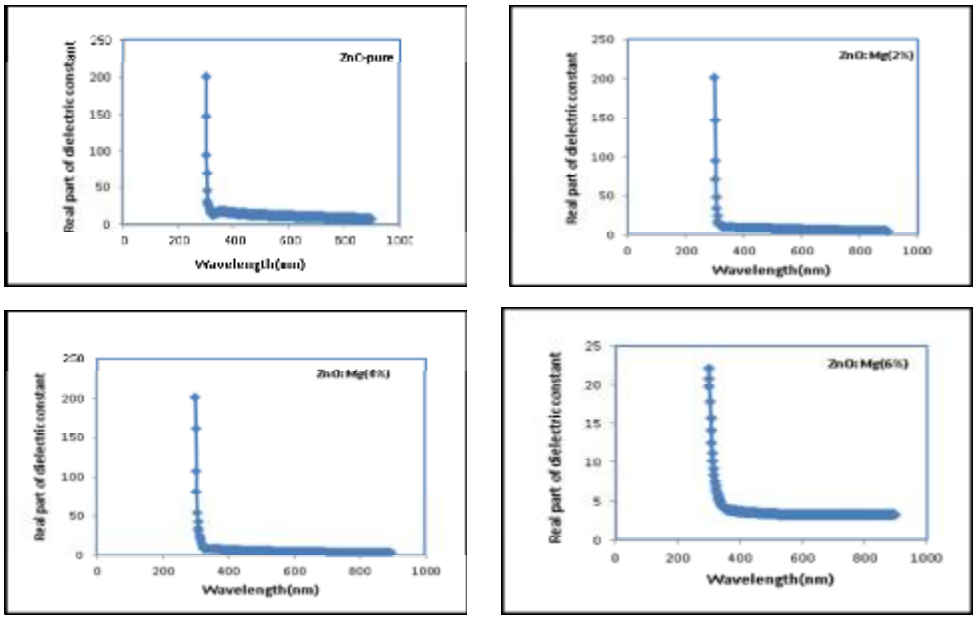

Figure. (13) Real part of dielectric constant of the $Mg_xZn_{1-x}O$ thin films.

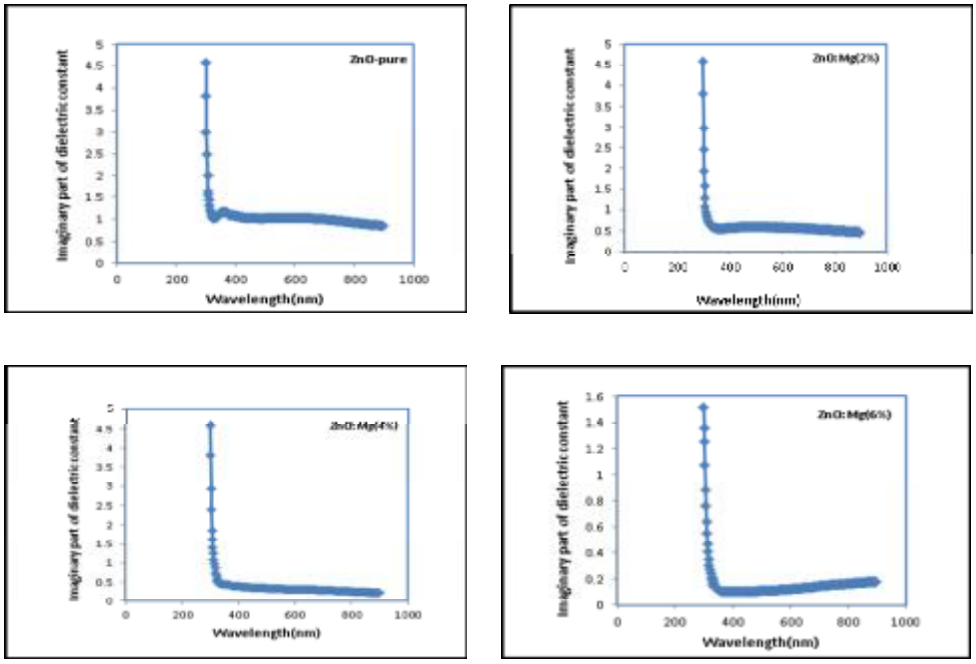

Figure. (14) Imaginary part of dielectric constant of the $Mg_xZn_{1-x}O$ thin films.

Optical Conductivity (σ)

Fig.(15) shows the variation of optical conductivity as a function of wavelength for different Mg-content of the $Mg_xZn_{1-x}O$ thin films. From Figures, we can see that the optical conductivity increases with increasing photon energy. This suggests that the increase in optical conductivity is due to electron exited by photon energy, and the optical conductivity of the films increases with increasing Mg-content in the films.

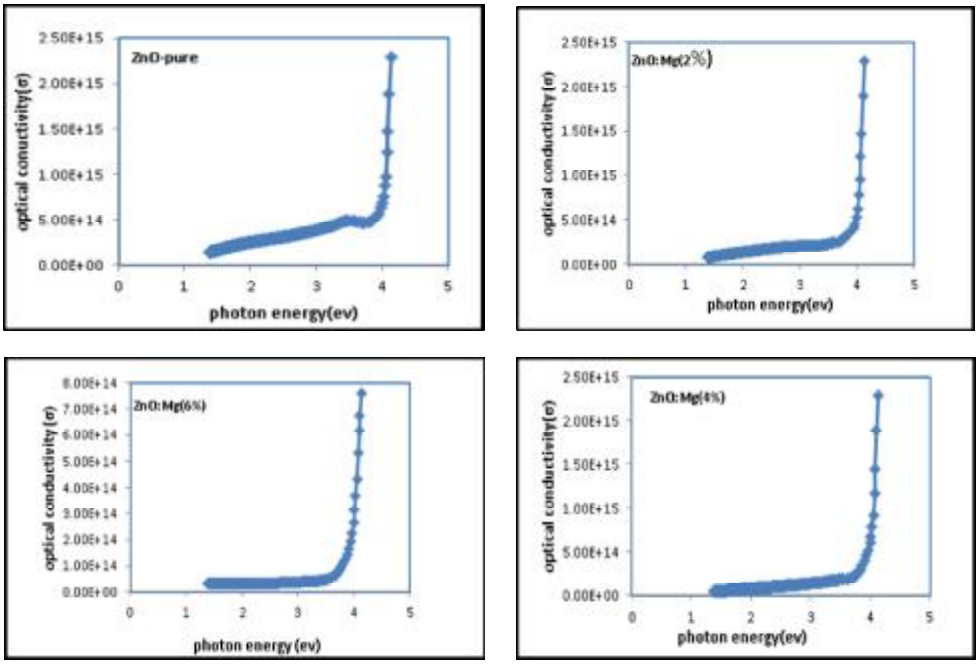

Figure.(15) Optical conductivity as a function of photon energy for $Mg_xZn_{1-x}O$ thin films.

Conclusions

- increases the toughness of the as deposited films.
- The films deposited from pure ZnO and 6 wt.% Mg doped ZnO targets at oxygen pressure of ($2x10^{-1}$) mbar, (400)^oC substrate temperature and laser fluency (400) mJ are good candidates for structural, morphology and optical properties.
- The structural of the ZnO films are found to be dependent on the films doped The increase of the dopant concentration into the target. The result of (X-ray) diffraction shows that all thin films (pure and doped) exhibit polycrystalline nature, and has the hexagonal wurtzite structure with preferential orientation in the direction [101] plane, The crystal structure of the nanostructure $Mg_xZn_{1-x}O$ films is hexagonal wurtzite and the films are highly oriented. The SEM studiy show that the obtain nanocrystalline $Mg_xZn_{1-x}O$ thin film prepared with (x=0.04 and 0.06) has better surfaces. The AFM results show the slow growth of nanocrystallite sizes for the as-grown films. The root mean square (RMS) is decreasing from 56.6 to 39.4 nm as the doped increased up to x= 0.06. XRD, AFM and SEM analysis shows that the prepared films are nanocrystalline thin films with estimated comparable grain sizes. Also, the grain size of the prepared nanocrystalline thin films in the range ~ (30-50

nm).

- The optical properties of $Mg_xZn_{1-x}O$ thin films show that the films have allowed direct transition. The average transmittance for all the films is over 90% in the wavelength range (300-900) nm and the transmittance in UV region increases with the increase of films doped. The optical band gap is dependent on the films doped, increasing in the doping percentage for Mg cause a increase in the optical band gap value, also the values of refractive index (n) of $Mg_xZn_{1-x}O$ films lie in the range of (1.5 - 2.6). This means that the film suitable for using as a antireflection coating and also suitable for solar cell applications.

References

[1] R.Y. Borseand V.T. Salunke.," Structural and Electrical Resistivity Study of Synthesized ZnO Thick Film Resistors," Volume 1, Issue 1, pp. 1-13, 2013.
[2] P.X. Gao et al. Adv. Funct. Mater. 2006. 16; 53.
[3] J.E. Beek et al. Adv. Mater. 2004. 1216.
[4] Z.L. Wang et al. Science. 2006. 312; 242.
[5] J. Goldberger et al. J. Phys. Chem. 2005, B 109; 9.
[6] J.K. Sheu et al. J. Tune, Appl. Phys. Lett. 2007. 90; 263511.
[7] Z. Zhang et al. Nano Lett. 2008. 8; 652.
[8] Y.Y. Noh et al. Appl. Phys. Lett. 2007. 91; 043109.
[9] Y.F. Hsu et al. J. Appl. Phys. 2008. 103; 083114.
[10] Ahirwar Vishnu P., Misra P. and Ahirwar G.," A Study on Structural and Optical Properties of $Mg_xZn_{1-x}O$ thin films using Pulsed Laser Deposition (PLD)", Research Journal of Physical Sciences, Vol. 1(4), 11-14, May (2013).
[11] H. Zhuang, J. Wang, H. Liu, J. Li and P. Xu "Structural and Optical Properties ZnO Nanowires Doped with Magnesium "ACTA PHYSICA POLONICA A,vol.119,No.6, (2011).
[12] D.X. Zhao, Y.C. Liu, D.Z. Shen, Y.M. Lu, J.Y. Zhang and X.W. Fan, J. Appl. Phys. 90 (2001) 5561.
[13] Ali A. Yousif, "Preparation and Construction of Efficient Nanostructures Dopant ZnO Thin Films Prepared by Pulsed Laser Deposition for Gas Sensor", Ph.D. Thesis, Dept. of phys., University of Al-Mustansiriya, (2010).
[14] R. Ayouchi, F. Martin, D. Leinen and J.R. Ramos-Barrado, "Growth of pure ZnO thin films prepared by chemical spray pyrolysis on silicon" J. Cryst. Growth 247 (2003) 497.
[15] W.I. Park, G.C. Yi and H.M. Jang, "Metal organic vapor-phase epitaxial growth and photoluminescent properties of $Zn_{1-x}Mg_xO(0 < x < 0.49)$ thin films" Appl. Phys. Lett. 79 (2001) 2022.
[16] S.chiarin, M. Goano and E.Bclloti,J.Quant.Elec.47, 661, (2011)
[17] M. salina, R.Ahmed, A.B.suriani and M.Rusop, "Band gap Alteration of transparent Zinc Oxide thin films with Mg Dopant", Transction on electrical and electronic materials,vol.13,No.2,pp.64-68,April 25,(2012)
[18] L. W. Ji, C. M. Lin, T. H. Fang, T. T. Chu, H. Jiang, W. S. Shi, C. Z. Wua, T. L. Chang, T. H. Meen and J. Zhong, Appl. Surf. Sci., 256 (2010) 2138.
[19] J. Huang and C. Liu ," The influence of magnesium and hydrogen introduction in sputtered zinc oxide thin films " Thin Solid Film 498 (2006) 152.
[20] A. Ashour , M.A. Kaid , N.Z. El-Sayed and A.A. Ibrahim ," Physical properties of ZnO thin films deposited by spray pyrolysis technique" Applied Surface Science 252 (2006) 7844.

[21] Adawiya J. Haidar & Gehan E.Simon, "Optical and Structure Properties of MgxZn1-xO Thin Films by Pulsed Laser Deposition"Eng. & Tech. Journal ,Vol.27, No. 14, (2009).

[22] X. Zhang , X. Li , T. Chen , J. Bian and Can Yun Zhang ," Structural and optical properties of $(Zn_{1-X}Mg_XO)$ thin films deposited by ultrasonic spray pyrolysis " Thin Solid Film 492 (2005) 248.

[23] B. J. Lokhande and M. D. Uplane, "Structural, optical and electrical studies on spray deposited highly oriented ZnO films" Appl. Surf. Sci. 167 (2000) 243.

[24] T.K. Subramanyam, B. Srinivasulu Naidu and S. Uthanna, "Structure and Optical Properties of dc Reactive Magnetron Sputtered Zinc Oxide Films"Cryst. Res. Technol. 34 (1999) 981.

[25] M.A. Martinez, J.J. Herrero and M.J. Gutierrez, "Properties of RF sputtered zinc oxide based thin films made from different targets" Sol. Energy Mater. Sol. Cells 31 (1994) 489.

[26] Y. Qu, T.A. Gessert, J.J. Coutts and R. Noufi, "Study of ion-beam-sputtered ZnO films as a function of deposition temperature" J. Vac. Sci. Technol. A1$_2$ (1994) 1507.

[27] T.Y. Ma, S.H. Kim, H.Y. Moon, G.C. Park, Y.J. Kim and K.W. Kim,"Substrate Temperature Dependence of ZnO Films Prepared by Ultrasonic Spray Pyrolysis" Jpn. J. Appl. Phys. 35 (1996) 6208

[28] S. Mathew, P.S. Mukerjee and K.P. Vijayakumar, "Optical and surface properties of spray-pyrolysed CdS thin films" Thin Solid Films 254 (1995) 278.

[29] U. Pal, R. Silva-Gonzalez, G. Martinez-Montes, M. Gracia-Jimenez, M.A. Vidal and Sh. Torres, "Optical characterization of vacuum evaporated cadmium sulfide films "Thin Solid Films 305 (1997) 345.